



Development and Characterization of Propylene Glycol Alginate –Folic Acid Conjugate Based Micelles Containing Erlotinib

Ashish Gorle, Anand Mundada, Pankaj Nerkar*, Nupur Baheti, Pooja Mundada

R C Patel Institute of Pharmaceutical Education and Research, Shirpur

(Received: 07 January 2024

Revised: 12 February 2024

Accepted: 06 March 2024)

KEYWORDS

lorem ipsum

ABSTRACT:

Introduction: Erlotinib (ERL) is an epidermal growth factor receptor type (HER-1) tyrosine kinase inhibitor, which has been approved for the treatment of metastatic advanced non-small cell lung (NSCLC) and pancreatic cancer.

Objectives: The present work aims to synthesize the conjugate of propylene glycol alginate-folic acid (PGA-FA) and employ it to prepare ERL-loaded micelles, using the thin film hydration method which is further evaluated in vitro and in vivo.

Methods: The conjugate was synthesized via a reaction of the carboxyl groups of folate with the amine groups of PGA and catalyzed by EDC (1-Ethyl-3-(3-dimethyl aminopropyl) carbodiimide) as an amide coupling agent. The prepared conjugates were characterized by ¹H NMR, DSC, XRD, SEM, and TEM. In vitro, the drug release profile was evaluated for ERL-loaded micelles using dialysis bag methods.

Results: The results showed that the drug was entrapped successfully within the hydrophobic core of the micelles. In the study, ERL-loaded micelles showed higher C_{max} (76.6754 ng/ml for IV) than free ERL (39.4079 ng/ml and 44.7574 ng/ml through the oral route and Intramuscular route, respectively) and higher AUC₀₋₂₄ (321.78797 ng/ml.h) than free drug (266.78127 ng/ml.h and 347.49328 for oral and IV respectively).

Conclusions: The present investigation revealed that ERL-functionalized micelles might be promising for delivering anti-cancer agents and improving their therapeutic efficacy.

1. Introduction

Propylene glycol alginate (PGA) is a high molecular weight linear polysaccharide composed of 1, 4 Linked-D-mannuronic acid (31%-65%) and L-guluronic acid (69%-35%). PGA is food grade polysaccharide ester of alginate and has beneficial properties like film forming, gelling, suspending, emulsifying, and stabilizing agents [1-4].

The US-FDA has approved erlotinib (ERL) for the treatment of metastatic advanced non-small cell lung (NSCLC) and pancreatic cancer, is an epidermal growth factor receptor (EGFR) type (HER-1) tyrosine kinase inhibitor [5, 6]. The tyrosine kinase inhibitors are a newer and novel class of anti-cancer drugs, predominantly for pancreatic cancer, which selectively bind to the ATP catalytic domain of HER-1 reversibly for attaching to the

adenosine triphosphate (ATP) binding site of the receptor and hence inhibits the EGF-induced phosphorylation and prevents the cell proliferation [7].

Polymeric micellar structures have led to the design and development of smart drug delivery systems (DDSs) to deliver various anti-cancer agents [8, 9].

2. Objectives

ERL has poor bioavailability when administered through the oral route, mainly due to its poor solubilities, instability in the gastrointestinal environment, and high first-pass metabolism [10, 11]. Various approaches have been evaluated to overcome the challenges associated with conventional ERL therapies [12]. Thus, there is scope for ERL molecules to form in novel injectable formulations, which could improve drug delivery of ERL



as an anti-cancer drug for targeting and maximizing the anti-cancer effect of the drug with minimal side effects [13]. Further, to increase the targeting efficiency of polymer to tumor cells specifically, PGA was conjugated with folic acid (FA) [14, 15, 16]. The present work aims to synthesize the conjugate of PGA-FA and employ it to prepare ERL micelles, which are further evaluated in vitro and in vivo.

3. Methods

Materials

ERL was obtained as a gratis sample from MSN Lab Pvt. Ltd, Hyderabad, India. Propylene glycol alginate (PGA) was purchased from Amit cellulose, Mumbai, India. EDC (1-Ethyl-3-(3-dimethylaminopropyl) carbodiimide) was purchased from Survival Technologies, Ankleshwar, India. Dialysis bag (MW cut off 12,000 Da) and folic Acid were purchased from Sigma Aldrich Chemical Private Ltd, Bangalore, India, and Loba Chemie Pvt. Ltd, Mumbai, India, respectively. Potassium iodide (KI), Iodine (I₂), methanol, and dimethyl sulfoxide (DMSO) were purchased from Merck Chemicals (Mumbai, India). All other solvents and reagents used were of analytical grades.

Synthesis of PGA-FA Conjugate

A 1-ethyl-3-(3-dimethylaminopropyl) carbodiimide (EDC) coupling reaction synthesized a PGA-FA conjugate. PGA-FA conjugate was synthesized via a reaction of the carboxyl groups of FA with the amine groups of PGA and catalyzed by EDC. In brief, the procedure consisted of 2 gm of Folic Acid dissolved in 25 mL of DMSO reacted with 1 gm of EDC at room temperature for 1 hour under stirring. The above reaction mixture was added to the 3% w/v conc. of propylene glycol alginate (PGA) solution which was prepared by dissolving 1.50 gm of PGA in 50 mL of distilled water. The resulting mixture was stirred at room temperature in the dark for 16 h [17]. The resulting mixture was dialyzed for 48h against distilled water to remove by-products, and the sample was then subjected to lyophilization to form a dry lyophilized powder.

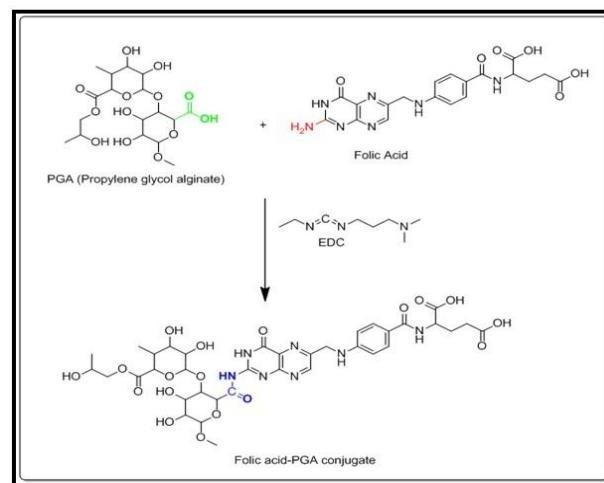


Figure 1- Synthesis of FA-PGA Conjugate

Characterization of PGA-FA conjugate

a. NMR

Proton NMR (¹H NMR) spectra of PGA, Folic Acid, and its Prepared PGA-FA Conjugate were recorded in DMSO using Bruker Avance-II 400 UltraShield™ spectrophotometer (with Bruker Avance-II Autosampler and Topspin 2.7 software). Tetramethylsilane (TMS) was used as a reference standard. Chemical shifts (δ) were expressed in ppm relative to TMS.

b. Fourier Transform Infra-red spectroscopy (FTIR)

The FT-IR spectra of Folic Acid, PGA, and the PGA-FA conjugate between 4000 cm⁻¹ and 450 cm⁻¹ (mid-infrared region) were obtained using an 8400S FTIR Shimadzu, Japan, equipped with IR Solution software. Each sample was prepared with a spectroscopic grade potassium bromide (KBr) powder and then pressed into pellets (1mg of sample per 100 mg dry KBr) [18].

Critical Micellar Concentration (CMC) determination of PGA-FA Conjugate

The well-reported iodine UV Spectroscopy method determined the CMC values of the PGA-FA Conjugate. A standard iodine solution was prepared by dissolving 0.5 gm of iodine and 1 gm of potassium iodide in 50 mL of distilled water. Various dilutions from the range of 1–16 μg/mL of the conjugate were prepared, and to each dilution, 25 μL of standard iodine solution was added. The resulting solutions were kept overnight in the dark and measured at a wavelength of 366 nm using UV–Visible spectrophotometer (UV 2450, Shimadzu, Japan).



The absorption intensity of iodine was plotted against the logarithm of polymer mass concentration, and CMC was determined from the graph. The sharp increase in iodine intensity indicates the formation of micelles [19, 20].

Preparation of ERL and PGA-FA loaded mixed micelles

The thin film hydration method was used to prepare ERL- PGA-FA loaded micelles (ERL- PGA-FA). Aqueous dispersions of ERL were prepared by dispersing 100 mg of ERL in 100 mL of distilled water containing 1.5% w/w of PGA-FA conjugate, the dispersion mixture was subjected to sonication (Sonorex ultrasonicator). Four batches of ERL-loaded polymeric micelles were prepared. The concentration of the drug in each batch was kept constant, whereas the concentration of prepared PGA-FA conjugate in each batch was changed in the range of 1.5% w/w, 2% w/w, 2.5 % w/w, and 3 % w/w were dissolved in 100 mL of water respectively for each batch. Distilled water was evaporated using a rotary evaporator (KNF LABS RC 600, Switzerland) at 37°C, and a thin film of drug-dispersed PGA was formed. The resulting film was re-suspended in about 50ml of distilled water. Then the sample was subjected to lyophilization to form dry lyophilized powder [21].

Particle size and surface charge

The Particle size, Polydispersity Index (PDI), and Zeta Potential of formulation were measured by dynamic light scattering technique, using Zetasizer (Nano ZS 90 Malvern Instruments, UK) at room temperature. The samples were suitably diluted with double distilled water before every measurement and sonicated for 5 min to ensure the solution was well dispersed [22].

Production Yield

The production yield of micelles of various formulations was calculated using the weight of final products after drying concerning the initial total weight of the drug and polymer used to prepare polymeric micelle [23].

Percentage drug loading (% DL) and percentage entrapment efficiency (% EE)

Percent entrapment efficiency (% EE) is defined as the percentage of drug incorporated into the polymeric nanoparticles relative to the total drug added. It specifies how much percent of the drug is included in the particles

and how much of the free drug is still present in the dispersion mediums. For this, micelles dispersion was centrifuged at 45,000 rpm for 35 min; 1.0 mL of the supernatant collected after centrifugation was diluted with methanol and then makeup volumes up to 10 ml in 10ml volumetric flask and measured spectrophotometrically at 246 nm using UV-Visible spectrophotometer (UV 2450, Shimadzu, Japan). The entrapment efficiency of the micelles was calculated for each batch of micelles[12, 24].

Scanning Electron Microscopy (SEM) and Transmission electron microscopy (TEM)

The shape and surface morphology of the micelles were visualized using scanning electron microscopy (Jeol 6390LV, Kochi). Samples were prepared by placing one drop of micelles solutions on a copper grid and then drying under vacuum pressure. The samples were examined using SEM at 10 kV [25, 26]. The surface morphology of ERL-loaded micelles was also studied by transmission electron microscope (JEM-2100, 200 kV, Jeol, SAIF, NEHU, Shillong). ERL-loaded micelle (1mg) was dispersed in distilled water. A drop was placed on the carbon-coated copper grid and stained with phosphotungstic acid (2% w/v). Finally, the grid was air-dried and scanned with TEM at different magnifications [26].

X-ray diffraction (XRD)

Powder X-ray diffraction (PXRD) patterns of ERL and the formulated micelles were recorded with an X-ray diffractometer (Bruker AXS Kappa APEX II CCD, Kochi) employing Cu K α (wavelength 1.5406 Å, tube operated at 40 kV, 40 mA) at room temperature. Data were collected over an angular range from 4 to 40° 2 θ at a 176-step size of 0.01° and a scan rate of one second.

In Vitro Drug Release

In vitro, the drug release profile was investigated for ERL-prepared micelles using dialysis bag methods. Dispersion of ERL-prepared micelles equivalent to 50 mg of ERL was filled in the dialysis bag and tied at both ends. The dialysis bag was immersed into a beaker containing 100 mL of PBS (pH 7.4) at 37°C with continuous magnetic stirring at 50 rpm/min. At predetermined time intervals (0.5- 6h) sample was withdrawn and replaced with an equal volume of fresh medium to maintain sink condition. The samples were



analyzed by UV-visible spectrophotometer (UV 2450, Shimadzu, Japan) at 246 nm. The % drug release and cumulative drug release were calculated [27]. The mechanism of drug release for ERL was evaluated by fitting the data in different mathematical models, e.g., zero order, first order, Higuchi kinetics, and Korsmeyer-Peppas model.

Pharmacokinetic study

Male Wistar Rats of 150–200 g was obtained from the central animal facility of the Institute. The Institutional Animal Ethics Committee (IAEC) approved the study protocol. The animals were maintained at $25 \pm 2^\circ\text{C}$ and 50–60% relative humidity (RH) under natural light/dark conditions. They were divided into three groups, each group containing Three rats ($n = 3$). Before the study, the animal fasted overnight for 12h with free access to water. Groups A, B, and C received a single oral, intravenous, and intravenous dose equivalent to 10 mg/kg of ERL dose. After mild ether anesthetization, serial blood samples were collected using a retro-orbital puncture technique at predetermined intervals (0.5- 24 h) in heparinized microcentrifuge tubes [10]. The blood samples were centrifuged at 3,000 rpm for 10 min to separate plasma. Collected plasma samples were stored at approximately -20°C until analysis. The plasma samples were quantified to estimate ERL through the previously developed HPLC method [12, 28-30]. Different pharmacokinetic parameters (e.g., Maximum concentration (C_{max}), time to reach maximum concentration (T_{max}), the area under concentrations–time curve (AUC), elimination half-life ($t_{1/2}$), and mean residence time (MRT)) of study samples were estimated by Kinetica software version 5.0 (Thermo Fisher Scientific Inc., USA), and compared with standard samples [12].

4. Results

Synthesis of PGA-FA Conjugate

The preparation procedure of PGA-FA was confirmed after consulting the literature [31]. PGA- FA conjugate was successfully synthesized by conjugation of folic acid via the reaction of the carboxyl groups of FA with the amine groups of PGA, catalyzed by EDC as an amide coupling agent. EDC activated the carboxyl groups of FA. The prepared conjugates were characterized by NMR, DSC, and FTIR.

Characterization of Prepared Conjugate

a. NMR

$^1\text{H-NMR}$ spectra of folic acid demonstrated hydrogens present in the structure of folic acid, as shown in Figure 2. $^1\text{H-NMR}$ spectra have shown broad peaks at 4.2δ ppm for methylene ($-\text{CH}_2-$) protons. $^1\text{H-NMR}$ spectra also displayed proton absorption singlet at 8.7δ ppm due to NH_2 protons. The proton absorption singlet was observed at 4.0δ ppm due to $-\text{NHCH}_2-$ protons. Aromatic hydrogens have appeared as multiplets at $6.7-$ 7.5δ ppm. $^1\text{H-NMR}$ spectra of propylene glycol alginate seemed as multiplets between 3.2 to 5.03δ ppm for all saturated hydrogens and hydroxyl groups (C-H and $-\text{OH}$) present in the compound. The presence of the methoxy ($-\text{OCH}_3$) group exhibited a peak in the $^1\text{H-NMR}$ spectrum around 3.5δ ppm. The peak appeared at a lower frequency of 1.3δ ppm and was assigned to methylene hydrogens, as shown in Figure 3. The reaction of the primary amino group of folic acid and propylene glycol in the presence of EDC was confirmed by $^1\text{H-NMR}$ of FA-PGA conjugate. The distinctive peak as a doublet was seen in all spectra of $^1\text{H NMR}$ for synthesized molecules in the range of $3.33-3.52 \delta$ ppm due to $-\text{N-CH}_2-\text{CO}$ linkage. For aliphatic amide, $^1\text{H-NMR}$ exhibited a characteristic peak around 4.05δ ppm, indicating the formation of the desired polymer. Aromatic protons were present as multiplets in the range of $7.10-8.41 \delta$ ppm, Figure 4.

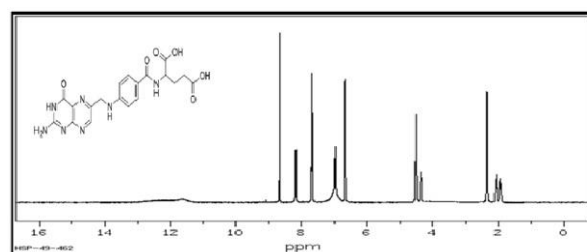


Figure 2 –NMR Spectra of Folic Acid

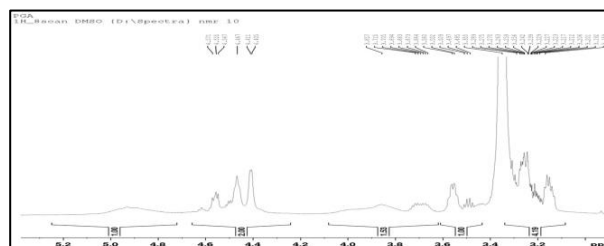


Figure3- NMR Spectra of Propylene glycol alginate

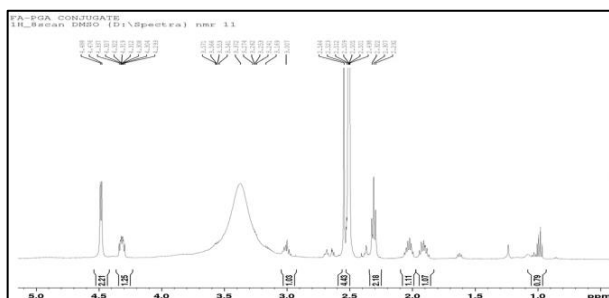


Figure 4: NMR Spectra of PGA- FA conjugate

b. FTIR Characterization of Folic Acid, PGA, and its conjugate

IR spectra have the presence of a representative band at 1597.11 cm⁻¹ for >C=O group of folic acid.

The IR spectrum of PGA exhibited bands at 2715.86 and 2374.45 cm⁻¹ for the presence of primary hydroxyl groups. Again, the presence of bands in the region of 2955.04 and 2928.04 cm⁻¹ are for methylene groups present in PGA. The conjugate of PGA-FA has been easily characterized by the appearance of multiple bands in regions 2955.04, 2928.04, and 2831.60 cm⁻¹ for aliphatic methylene groups stretching. The characteristic peak has appeared for carboxyl acid (-COOH) at 3446.91 cm⁻¹. The peak indicating conjugate formation through amide linkage (-CONH-) occurred around 1597.11 cm⁻¹. The FTIR spectra of folic acid-PGA conjugate are illustrated in Figure 5.

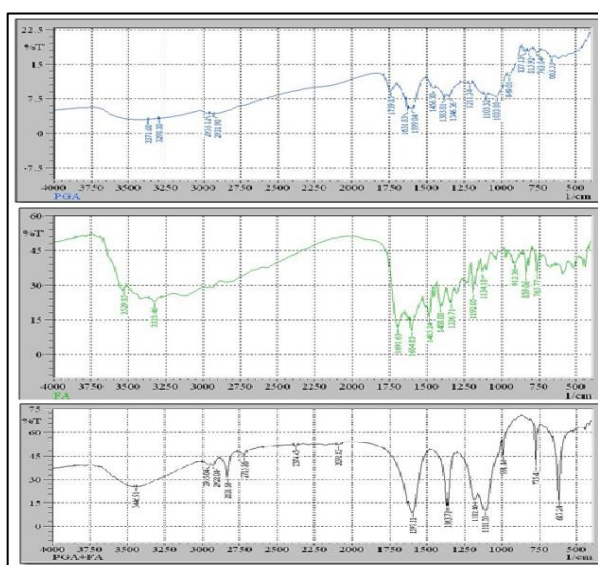


Figure 5: FTIR Spectra of propylene glycol alginate, folic Acid, and PGA-FA conjugate

CMC Determination

In the iodine UV spectroscopy method, the formation of micelles was monitored by using iodine (I₂) as a hydrophobic probe. Solubilized I₂ prefers to participate in the hydrophobic microenvironment of amphiphilic polymers, causing the conversion of I₃ to I₂ from the excess KI in the solution to maintain the saturated aqueous concentration of I₂ [32]. For the determination of CMC, I₂ absorbance intensity has been plotted as a function of polymer concentration, and the sharp increase in I₂ intensity against polymer concentration confirms the formation of micelles. After carrying out the study, it was concluded that PGA-FA leads to the formation of stable micelles in an aqueous medium at a considerably lower concentration of about 1.5%.

Preparation of ERL-loaded P-GA-FA conjugate-based micelles

Thin film hydration methods developed ERL-loaded PGA-FA conjugate-based micelles [21]. Different ratios of PGA-FA conjugate, i.e., 1.5% w/w, 2% w/w, 2.5% w/w, and 3% w/w, respectively, were used in each batch.

Particle size, PDI, Zeta potential, Production yield, Drug loading, and Entrapment Efficiency

The particle size, PDI, Zeta potential, Production yield, drug loading, and entrapment efficiency of four batches, i.e., F1, F2, F3, and F4 shown in Table 1.

Table 1: Particle size, Polydispersity index, Zeta Potential of ERL micelles.

S r. No.	Batch	Particle Size(d. nm)	Zeta Potential (mV)	PDI	Entrapment efficiency (%)	Drug loading (%)
1	F1	478	-27.0	0.638	92.74	75
2	F2	410	-23.9	0.495	92.70	74.21
3	F3	476	-18.9	0.610	95.20	81.6
4	F4	445	-14.5	0.334	95.57	88.05



SEM and TEM

SEM images of ERL-loaded micelles are shown in Figure 6 (A, B). SEM image of ERL loaded micelles showed irregular rectangular flake-like or flake-like shape with complete loss of its characteristic shape. The TEM images of ERL-loaded micelles (with different magnifications) were illustrated in Figure 6 (C, D).

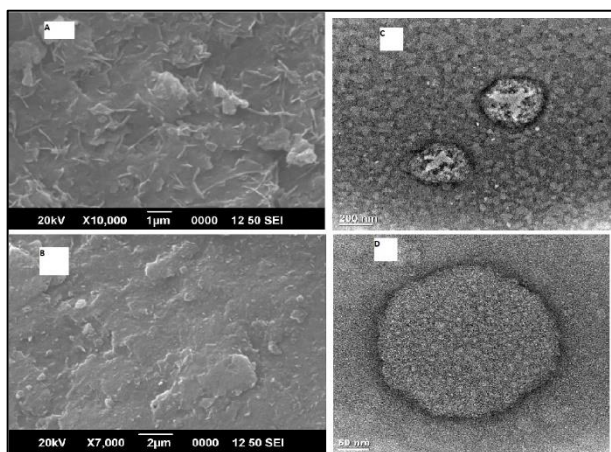


Figure 6: SEM image (A, B) of PGA-FA conjugate and TEM image of (C, D)

XRD

X-ray diffraction of drug and drug-loaded micelles was presented in Figure 7. The XRD pattern of ERL showed the presence of intense, sharp peaks at 7.267 on the 2θ scale, which indicated its crystalline structure. The formulated micelles showed crystalline peaks of ERL with reduced intensities.

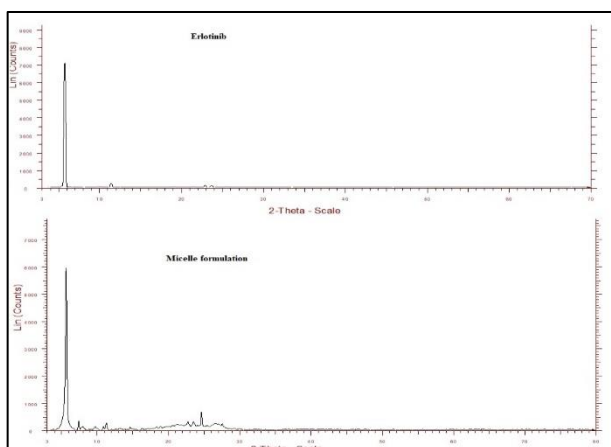


Figure 7: X-ray diffractograms of (A) pure ERL and (B) ERL-loaded Micelles based on PGA-FA conjugate

In-vitro drug release

The in-vitro drug release profiles of the ERL-loaded micelles with folic acid conjugation in PBS pH 7.4 for six hrs. by dialysis bag method are shown in Figure 8.

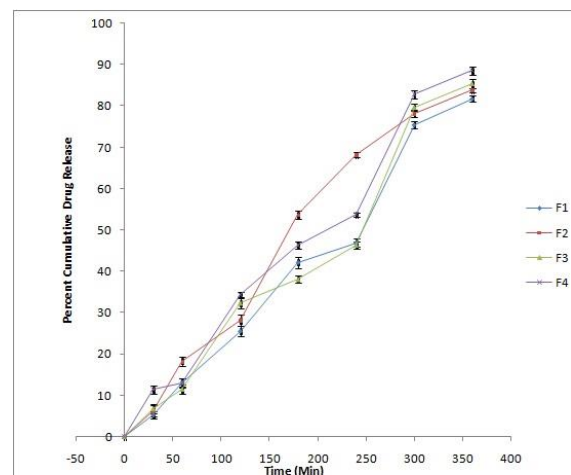


Figure 8: In vitro Drug release from various PGA-FA-based formulations

In vivo pharmacokinetics Parameters

Different pharmacokinetic parameters are listed in Table 2. In the study, ERL-loaded micelles showed higher Cmax (76.6754 ng/ml for IV) than free ERL (39.4079 ng/ml and 44.7574 ng/ml through the oral route and Intramuscular route, respectively) and higher AUC₀₋₂₄ (321.78797 ng/ml.h) than free drug (266.78127 ng/ml.h and 347.49328 for oral and IV respectively).

Table 2: Pharmacokinetic parameters of erlotinib formulations

Parameters	Oral Administration of ERL	IV Administration of ERL	IV Administration of F4 formulation
Cmax (ng/ml)	39.4079±5.12	44.7574±4.14	76.6754±4.25
Tmax (h)	1.5	-	0.5
AUC 0-	266.78127	347.49328	321.78797



24 h (ng/ml* h)	±11.28	±19.25	±10.12
Absolute bioavailability (Fabs)	76.77%	100%	92.60%

Discussion:

In the present study the conjugate of PGA and FA was synthesized and confirmed by NMR, FTIR technique. The amphiphilic nature of the conjugate was characterized by CMC determination. The CMC of the conjugate was observed to be 1.5 % (w/v). Film hydration method was used to prepare the ERL loaded micelles. Four formulations prepared contained increasing concentration of PGA-FA (1.5% -3.0 %). All formulations were invitro evaluated. The particle size of four formulations was in the range of 410-478 nm. The zeta potential was observed to be anionic in nature which may be credited to the unchanged anionic nature of PGA. Drug loading and entrapment efficiency was also determined for all formulations.

The surface morphology of the micelles was studied using SEM and TEM studies. SEM image of ERL loaded micelles showed irregular shape which further indicated the inclusion phenomenon between drug and micellar structure with the loss of crystallinity of drug. ERL-loaded micelles appeared as uniform spherical structure morphology unaffected by drug encapsulation. And show the dim ring of the polymeric core. In the figure, it can be observed that prepared nano micelles were well identified with spherical-shaped morphology.

X-ray diffractograms illustrated the crystalline nature of the drug. After loading the drug into the micelles, all characteristic sharp peaks are subdued due to the change into an amorphous state, suggesting complete drug entrapment into the micellar structure.

Drug release studies were found to be precise and followed the Higuchi's model with non-fickian transport. From Formulation F1 to F4, 82.29 to 89.58 % drug release was observed in 6 hrs. From the release profile, it was clear that the significantly higher and faster release of ERL from micelles.

The study showed that ERL-loaded micelles formulation increased the Cmax and AUC0 more efficiently than that of pure ERL drug. The prepared micelles formulation's absolute bioavailability was approximately high compared to pure ERL, further confirming the enhanced bioavailability of ERL-loaded micelles. These results revealed that micelles had a much higher rate and extent of bioavailability than pure ERL.

Conclusion

The present work highlighted PGA-FA conjugate synthesis and its application in the preparation of micelles and ERL loading in developed micelles. In this study, the reaction between the carboxyl groups of folate and the amine groups of PGA in the presence of EDC was carried out. The formulation of PGA-FA conjugate-based ERL-loaded micelles was successfully developed by the thin film hydration method and implemented to enhance the bioavailability of ERL. FT-IR, XRD, SEM, and TEM results show that the drug was entrapped successfully within the hydrophobic core of the micelles. To sum up, the experimental results of in vitro and in vivo showed that folic acid functionalized ERL-loaded micelles performed well in in-vitro and in-vivo characterizations. The present investigation revealed that ERL-loaded micelles might be promising for delivering anti-cancer agents which are hydrophobic in nature and to improve their therapeutic efficacy.

Acknowledgement

The authors are thankful to the Principal and Management of R C Patel Institute of Pharmaceutical Education and Research, Shirpur, for providing all necessary help and facilities to successfully carry out this research work.

Funding:

Not applicable

Availability of data and materials:

All data and materials are available on request.

List of Abbreviations

% DL – Percent Drug Loading

% EE – Percent Entrapment Efficiency

ATP - Adenosine Triphosphate

AUC – Area Under Curve



C_{max} - Maximum Concentration

CMC - Critical Micellar Concentration

DDS - Drug Delivery Systems

DMSO - Dimethyl Sulfoxide

EDC - 1-Ethyl-3-(3-dimethyl aminopropyl) carbodiimide

EGFR - Epidermal Growth Factor Receptor

ERL - Erlotinib

FTIR - Fourier Transform Infra-Red Spectroscopy

gm - Gram

I₂ - Iodine

KBr - Potassium Bromide

kV - Kilo Volts

mg - Milligram

mL - milliliter

NMR - Nuclear Magnetic Resonance

NSCLC - Non-Small Cell Lung

oC - Degree Celsius

PBS - Phosphate Buffer Saline

PDI - Polydispersity Index

PGA - Propylene Glycol Alginate

PGA-FA - Propylene Glycol Alginate and Folic Acid Conjugate

ppm - Parts Per Million

PXRD - Powder X-ray Diffraction

SEM - Scanning Electron Microscopy

TEM - Transmission Electron Microscopy

T_{max} - Time to peak drug concentration

TMS - Tetramethylsilane

US-FDA - United States Food Drug Administration

XRD - X-Ray Diffraction

References

- Sun, C., Dai, L., & Gao, Y. (2017). Formation and characterization of the binary complex between zein and propylene glycol alginate at neutral pH. *Food Hydrocolloids*, 64, 36–47.
- Li, G., Zhao, Y., Zhang, J., Hao, J., Xu, D., & Cao, Y. (2022). CaCO₃ loaded lipid microspheres prepared by the solid-in-oil-in-water emulsions technique with propylene glycol alginate and xanthan gum. *Frontiers in Nutrition*, 9.
- Xi, C., Sun, Z., Chen, X., Ding, X., & Zhang, T. (2022). Characterization of coacervation behavior between whey protein isolate and propylene glycol alginate: A morphology, spectroscopy, and thermodynamics study. *Food Chemistry: X*, 15, 100402.
- Moroni, A., Drefko, W., & Thone, G. (2011). Formulations of zero-order, pH-dependent, sustained release matrix systems by ionotropic gelation of alginate-containing mixtures. *Drug Development and Industrial Pharmacy*, 37(2), 216–224.
- Steins, M., Thomas, M., & Geißler, M. (2018). Erlotinib. *Small Molecules in Oncology*, 1–17.
- Pandey, P., & Dureja, H. (2018). Erlotinib in non-small cell lung cancer: from a thought to necessity. *Clinical Cancer Drugs*, 5(2), 87–93.
- Latha, S. T., Thangadurai, S. A., Jambulingam, M., Sereya, K., Kamalakannan, D., & Anilkumar, M. (2017). Development and validation of RP-HPLC method for the estimation of Erlotinib in pharmaceutical formulation. *Arabian Journal of Chemistry*, 10, S1138--S1144.
- Ghosh, B., & Biswas, S. (2021). Polymeric micelles in cancer therapy: State of the art. *Journal of Controlled Release*, 332, 127–147.
- Khan, S., Vahdani, Y., Hussain, A., Haghghat, S., Heidari, F., Nouri, M., Bloukh, S. H., Edis, Z., Babadaei, M. M. N., Ale-Ebrahim, M., & others. (2021). Polymeric micelles functionalized with cell penetrating peptides as potential pH-sensitive platforms in drug delivery for cancer therapy: A review. *Arabian Journal of Chemistry*, 14(8), 103264.
- Dora, C. P., Trotta, F., Kushwah, V., Devasari, N., Singh, C., Suresh, S., & Jain, S. (2016). Potential of erlotinib cyclodextrin nanosponge complex to enhance solubility, dissolution rate, in vitro cytotoxicity and oral bioavailability. *Carbohydrate Polymers*, 137, 339–349.
- Jain, S., Dongare, K., Nallamothe, B., Dora, C. P., Kushwah, V., Katiyar, S. S., & Sharma, R. (2022).



- Enhanced stability and oral bioavailability of erlotinib by solid self nano emulsifying drug delivery systems. *International Journal of Pharmaceutics*, 622, 121852.
12. Rampaka, R., Ommi, K., & Chella, N. (2021). Role of solid lipid nanoparticles as drug delivery vehicles on the pharmacokinetic variability of Erlotinib HCl. *Journal of Drug Delivery Science and Technology*, 66, 102886.
13. Deshmukh, T. V., Doijad, R. C., & Yadav, A. V. (2019). Polycaprolactone based Injectable Microspheres of Erlotinib Hydrochloride for Sustained Release: Optimization using Factorial Design. *Journal of Current Pharma Research*, 9(3), 3174–3191.
14. Jia, L., Li, Z., Zheng, D., Li, Z., & Zhao, Z. (2021). A targeted and redox/pH-responsive chitosan oligosaccharide derivatives based nanohybrids for overcoming multidrug resistance of breast cancer cells. *Carbohydrate Polymers*, 251, 117008.
15. Niu, L., Zhu, F., Li, B., Zhao, L., Liang, H., Yan, Y., & Tan, H. (2018). Folate-conjugated and pH-triggered doxorubicin and paclitaxel co-delivery micellar system for targeted anticancer drug delivery. *Materials Chemistry Frontiers*, 2(8), 1529–1538.
16. Scaranti, M., Cojocaru, E., Banerjee, S., & Banerji, U. (2020). Exploiting the folate receptor α in oncology. *Nature Reviews Clinical Oncology*, 17(6), 349–359.
17. Hao, J., Tong, T., Jin, K., Zhuang, Q., Han, T., Bi, Y., Wang, J., & Wang, X. (2017). Folic acid-functionalized drug delivery platform of resveratrol based on Pluronic 127/D- α -tocopheryl polyethylene glycol 1000 succinate mixed micelles. *International Journal of Nanomedicine*, 12, 2279.
18. Mohammed, A.-S. Y., Dyab, A. K. F., Taha, F., & Abd El-Mageed, A. I. A. (2021). Encapsulation of folic acid (vitamin B9) into sporopollenin microcapsules: physico-chemical characterisation, in vitro controlled release and photoprotection study. *Materials Science and Engineering: C*, 128, 112271.
19. Patil, S. S., Chougale, R. D., Manjappa, A. S., Disouza, J. I., Hajare, A. A., & Patil, K. S. (2022). Statistically developed docetaxel-laden mixed micelles for improved therapy of breast cancer. *OpenNano*, 8, 100079.
20. Hajare, A., Dol, H., & Patil, K. (2021). Design and development of terbinafine hydrochloride ethosomal gel for enhancement of transdermal delivery: In vitro, in vivo, molecular docking, and stability study. *Journal of Drug Delivery Science and Technology*, 61, 102280.
21. Nasr, M., Hashem, F., Abdelmoniem, R., Tantawy, N., & Teiama, M. (2020). In vitro cytotoxicity and cellular uptake of tamoxifen citrate-loaded polymeric micelles. *AAPS PharmSciTech*, 21, 1–11.
22. S.Mupkalkar, N. Kommineni, Design and Characterization of erlotinib nanoparticles. *IJMR*, 7 (2021)1-1. DOI: 10.36713/epra2013
23. Mahajan, H. S., & Mahajan, P. R. (2016). Development of grafted xyloglucan micelles for pulmonary delivery of curcumin: in vitro and in vivo studies. *International Journal of Biological Macromolecules*, 82, 621–627.
24. Bera, H., Ang, S. R., Chiong, S. W., Chan, C. H., Abbasi, Y. F., Law, L. P., Chatterjee, B., & Venugopal, V. (2020). Core-shell structured pullulan based nanocomposites as erlotinib delivery shuttles. *International Journal of Polymeric Materials and Polymeric Biomaterials*, 69(13), 848–859.
25. Iizhar, S. A., Syed, I. A., Satar, R., & Ansari, S. A. (2016). In vitro assessment of pharmaceutical potential of ethosomes entrapped with terbinafine hydrochloride. *Journal of Advanced Research*, 7(3), 453–461.
26. Bera, H., Abosheasha, M. A., Ito, Y., & Ueda, M. (2021). Etherified pullulan-polyethylenimine based nanoscaffolds improved chemosensitivity of erlotinib on hypoxic cancer cells. *Carbohydrate Polymers*, 271, 118441.
27. Liu, X., Chen, Y., Chen, X., Su, J., & Huang, C. (2019). Enhanced efficacy of baicalin-loaded TPGS polymeric micelles against periodontitis. *Materials Science and Engineering: C*, 101, 387–395.
28. van Veelen, A., van Geel, R., Schoufs, R., de Beer, Y., Stolk, L. M., Hendriks, L. E. L., & Croes, S. (2021). Development and validation of an HPLC--MS/MS method to simultaneously quantify alectinib, crizotinib, erlotinib, gefitinib and osimertinib in human plasma samples, using one assay run. *Biomedical Chromatography*, 35(12), e5224.
29. Ramachandran, D., Ramakrishna, V. S., Bharath, P., & Jogarao, Y. (2022). Development & Validation of



RP-HPLC Method for Quantitative Estimation of Dasatinib and its Impurities in Pharmaceutical Dosage Form. *Journal of Pharmaceutical Research International*, 52–65.

30. Amirtharaj, R. V., & Lavanya, S. (2021). Development and validation of RP-HPLC and UV method for erlotinib hydrochloride tablets. *IP International Journal of Comprehensive and Advanced Pharmacology*, 6(3), 144–151. <https://doi.org/10.18231/j.ijcaap.2021.026>
31. Li, W., Xu, C., Li, S., Chen, X., Fan, X., Hu, Z., Wu, Y.-L., & Li, Z. (2019). Cyclodextrin based unimolecular micelles with targeting and biocleavable abilities as chemotherapeutic carrier to overcome drug resistance. *Materials Science and Engineering: C*, 105, 110047.
32. Patil, K. S., Hajare, A. A., Manjappa, A. S., More, H. N., & Disouza, J. I. (2022). Design, Development, In Silico, and In Vitro Characterization of Camptothecin-Loaded Mixed Micelles: In Vitro Testing of Verapamil and Ranolazine for Repurposing as Coadjuvant Therapy in Cancer. *Journal of Pharmaceutical Innovation*, 1–19.